



Improved sensitivity in indirect monitoring of chemical shifts of proton-heteronuclear spin pairs (^1H - ^{13}C and ^1H - ^{15}N) in 3D and 4D NMR spectroscopy

Renzo Bazzo*, Gaetano Barbato & Daniel O. Cicero

IRBM, Istituto di Ricerche di Biologia Molecolare P. Angeletti, Via Pontina Km.30.600, I-00040 Pomezia (Roma), Italy

Received 29 September 2000; Accepted 22 December 2000

Key words: 4D spectroscopy, HMQC, HSQC, protein NMR, sensitivity enhancement

Abstract

In three-dimensional and four-dimensional experiments on doubly labelled proteins not only heteronuclear (^{13}C or ^{15}N) but also proton (^1H) frequencies are often indirectly monitored, rather than being directly observed. In this communication we show how in these experiments by overlaying ^1H and heteronuclear evolutions one can obtain decreased apparent relaxation rates of ^1H signals, yielding improved sensitivity. The new method applies to spin pairs like ^1H - ^{15}N , as in amide groups, or ^1H - ^{13}C , as in methine groups of alpha or aromatic systems.

Heteronuclear correlation pulse sequences involving either single quantum (HSQC) or multiple quantum (HMQC) coherences are often used in high-resolution NMR as building blocks of three-dimensional and four-dimensional experiments in which not only heteronuclear but also proton frequencies are indirectly monitored, rather than being directly observed. Usually proton (t_1) and carbon (t_2) or proton (t_1) and nitrogen (t_2) are separately monitored, before an additional step of coherence transfer, typically via a proton-proton NOE, is executed. In this communication we show how sensitivity can be improved at the quite affordable cost of a more painstaking timing of the r.f. pulses in the sequence, without any substantial alteration of the rationale of the experiments.

In HMQC-NOESY experiments, the proton evolution time is currently implemented simply by increasing a given time interval that is subject to unavoidable T_2 relaxation losses (Fesik and Zuiderweg, 1988; Vuister et al., 1993). Indeed, to reduce such losses, a method known as 'semi-constant' time incrementation (Grzesiek and Bax, 1993) has long ago been introduced to take advantage of fixed delays inherently

present in the sequence, by gradually incorporating them in the appropriate evolution time. A more recent application has been illustrated for a 3D ^{13}C F_1 -edited, F_3 -filtered HMQC-NOESY (Lee et al., 1994), and these methods are now becoming more and more widespread.

In this communication we propose not only to exploit systematically all available fixed delays to monitor proton chemical shift evolution, but we extend the concept and show that also the heteronuclear incremented time can be exploited for the same purpose. Our target is to restrict the period in which protons undergo T_2 relaxation to the duration strictly necessary to obtain the desired resolution. To this effect the progressive overlaying of ^1H and heteronucleus evolution times in the course of the experiment can be used to provide a decreased apparent relaxation rate of ^1H signals. For ^1H T_2 values of the order of a few milliseconds, typical of macromolecules in solution, the advantage turns out to be largely worth the effort.

Figure 1 illustrates the pulse sequence for recording H(t_1)-C(t_2) HMQC-NOE-NH (t_3 detected) with the new method. As indicated, all three proton inversion pulses are progressively shifted to achieve t_1 evolution, until the available interval is fully exploited

*To whom correspondence should be addressed. E-mail: renzo_bazzo@merck.com

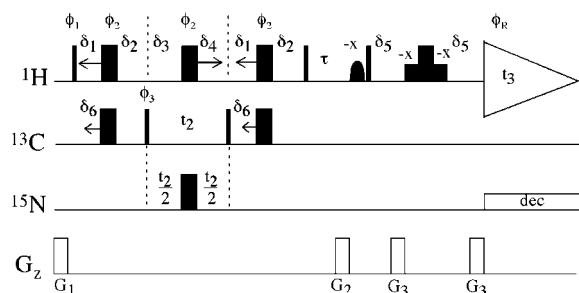


Figure 1. Pulse scheme for the 3D ¹H-¹³C HMQC-NOESY experiment. Narrow and wide pulses denote 90° and 180° flip angles, respectively. Pulse phases are along the x-axis unless indicated otherwise. $\phi_1 = 45^\circ, 45^\circ, 225^\circ, 225^\circ$; $\phi_2 = 135^\circ, 135^\circ, 315^\circ, 315^\circ$; $\phi_3 = 0^\circ, 180^\circ$; $\phi_k = 0^\circ, 180^\circ, 180^\circ, 0^\circ$; neglecting pulse duration in the following: $t_1 = -2\delta_1 + 2\delta_2 + \delta_3 - \delta_4$; $\Delta t_1 = 1/SW(F_1)$; $\Delta t_2 = 1/SW(F_2)$ (where SW denotes the sweep width); δ_1 (init.) = δ_2 (init.) = δ_6 (init.) = 1.5 ms; δ_3 (init.) = δ_4 (init.) = $t_2/2$; t_2 (init.) = 50 μ s; $\Delta t_1 = -2\Delta\delta_1 + 2\Delta\delta_2 + \Delta\delta_3 - \Delta\delta_4$; $\Delta\delta_1 = -1.5 \text{ ms}/(l_1 - 1)$; $\Delta\delta_3 = 0.5t_2/(l_1 - 1)$; $\Delta\delta_4 = -\Delta\delta_3$; $\Delta\delta_2 = \Delta t_1/2 + \Delta\delta_1 - \Delta\delta_3$; $\Delta\delta_6 = \Delta\delta_1$ for $(\delta_1 + \delta_2) < 3.7$ ms; $\Delta\delta_6 = \Delta\delta_1 + (\Delta\delta_2 + \Delta\delta_1)/2$ for $(\delta_1 + \delta_2) > 3.7$ ms; where t_1 and Δt_1 denote ¹H evolution time and its increment, respectively; and analogously for δ_i and $\Delta\delta_i$ with $\Delta\delta_i > 0$ for increment and $\Delta\delta_i < 0$ for decrement; $\Delta\delta_i$ values are functions of the current value of t_2 ; l_1 and l_2 are the number of complex data points for ¹H (F_1) and ¹³C (F_2), respectively. Gradient pulses are sine-bell shaped with maximum strength of 20 G/cm and duration: $G_1 = G_2 = 2$ ms; $G_3 = 0.4$ ms.

(i.e. until the first inversion pulse reaches a position immediately following the first 90° pulse and the second and third ones a back-to-back situation). Clearly, time incrementation will have to be implemented in a different way for different t_2 values. For short t_2 periods the different time intervals are incremented (or decremented) in such a way as to increase in parallel the duration of the intervals comprising the first ($\delta_1 + \delta_2$) and the third ($\delta_1 + \delta_2$) proton inversion pulses, until the maximum value for t_1 is reached. The corresponding carbon inversion pulses are shifted independently to maintain the same net heteronuclear coupling evolution time. Clearly, for short t_2 values the central delay ($\delta_3 + \delta_4$) can only be marginally relevant. In contrast, for long t_2 periods like towards the end of carbon t_2 evolution, the central delay can very significantly contribute. In the corresponding standard experiment (Lee et al., 1994) the central proton inversion pulse is kept fixed and therefore the whole t_2 period is not used for t_1 evolution, although proton magnetization happens to be in the transverse plane. In our new scheme the carbon t_2 period is fully included in the t_1 monitoring, by defining the delay increments and decrements in the pulse sequence as proper functions of the current t_2 duration. As the evolution time

t_2 is incremented to allow ¹³C frequency monitoring, the t_1 data point corresponding to a given net value of proton evolution is accomplished by different optimized arrangements of proton pulses and delays to minimize the total delay experienced by proton transverse magnetization. As a result of such a trick, the signal decay during t_2 is artificially slowed down as the t_1 evolution time is incremented. The corresponding peak-integrated intensities remain unaltered with respect to the conventional experiment, but the corresponding F_2 line-widths tend to be narrower for longer t_1 periods, since they benefit from an increasingly advantageous compensation as t_1 proceeds. An entirely symmetrical argument could be given for the signal decay in t_1 for any given t_2 data point. The result is indeed a modification of the theoretical 2D absorption Lorentzian peak shape in any F_3 - F_2 or F_3 - F_1 planes, in that some signal intensity in the F_2 or F_1 dimension is subtracted from the peak sides and pushed towards the centre. The result is a narrower peak with the same integral, and therefore an increased signal to noise ratio with respect to the corresponding peak of the conventional experiment. Broader peaks, corresponding to shorter relaxation times, will benefit to a greater extent and exhibit a greater sensitivity enhancement. In practice, however, the final outcome is a combined effect of ¹H and ¹³C relaxation, the duration of t_1 and t_2 evolution and the weighting function adopted in the data processing. If one adopts a shifted ($\pi/3$) sine-bell function, as in our case, the line shape is essentially determined by the apodization factor and the only detectable change is the sensitivity enhancement. For protons with T_2 values in the range 5–20 ms the signal enhancement turned out to be between 55% and 5% under the resolution conditions used.

The practical conditions for the new experiment can be selected as follows. At first the desired (or affordable) resolution is chosen for the F_2 heteronuclear dimension, by setting the maximum duration of the evolution time t_2 . This choice is clearly dictated by the persistence of an observable signal at the very end of the pulse sequence. However, it will also determine the time that is available, without further T_2 relaxation losses, for ¹H t_1 evolution. The latter, in fact, corresponds to the maximum duration of t_2 plus the duration of the two coherence transfer steps flanking it, from proton single quantum (SQ) to multiple quantum (MQ) coherences and back. Such an arrangement usually guarantees an optimized proton resolution with minimum relaxation losses. The comparison between the new scheme and the standard HMQC-NOESY se-

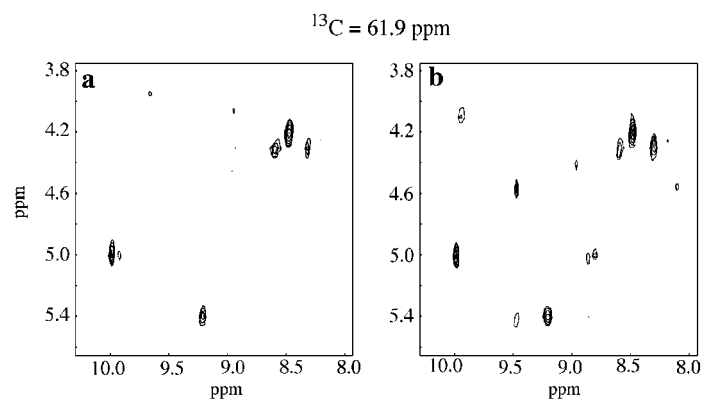


Figure 2. ${}^1\text{H}(\text{F}_1)\text{-}{}^1\text{H}(\text{F}_3)$ planes selected at the indicated ${}^{13}\text{C}$ chemical shift extracted from the 3D data sets obtained with the conventional pulse sequence (a) and with the new scheme (b), respectively. Total evolution times: ${}^1\text{H}$ $t_1 = 12.5$ ms; ${}^{13}\text{C}$ $t_2 = 5.3$ ms. In both the t_1 and t_2 dimensions a shifted $(\pi/3)$ sine-bell shaped weighting function has been applied prior to FT transformation. NOESY mixing time $\tau = 100$ ms.

quence was made by acquiring the two experiments on a sample of a complex between the protease domain of HCV NS3, a protein of 21 kDa (Barbato et al., 1999), and a peptide ligand. The spectra were recorded at room temperature using a Bruker AVANCE 600 MHz spectrometer. The sample concentration was 0.6 mM in 90% H_2O , 10% D_2O , pH 6.6. The experimental duration was 16 h. The advantage in terms of sensitivity gains due to reduced T_2 relaxation losses is illustrated in Figure 2, which shows the same $\text{H}(\text{F}_1)\text{-H}(\text{F}_3)$ plane (at ${}^{13}\text{C}$ (F_2) = 61.9 ppm) out of the 3D data sets obtained with the standard (a) and the new (b) pulse sequence. Proton signals with less favourable T_2 values are more penalized in the standard experiment and are clearly detected only with the new scheme.

In the HSQC-NOESY building block, used for example in the 4D ${}^{15}\text{N}\text{-}{}^1\text{H}\text{-NOE}\text{-}{}^{15}\text{N}\text{-}{}^1\text{H}$, only the time of the retro-INEPT preceding the NOE mixing is currently included in t_1 , adopting a semi-constant time incrementation (Grzesiek et al., 1995). Figure 3 illustrates our new pulse sequence for recording $\text{H}(t_1)\text{-N}(t_2)$ HSQC-NOE-NH (t_3 detected) in which ${}^1\text{H}$ evolution is accomplished in three consecutive steps. The initial t_1 increments are executed by right shifting the inversion pulse of the retro-INEPT until delay δ_5 approaches zero. This portion of the ${}^1\text{H}$ evolution can be performed in constant time ($\delta_4 + \delta_5 = 5.5$ ms) or in semi-constant time (extending for instance $\delta_4 + \delta_5$ from 4.5 ms to 5.5 ms) fashion. At this point ${}^1\text{H}$ evolution is continued by including the current duration of the ${}^{15}\text{N}$ t_2 evolution time in the t_1 period. To this purpose, since ${}^1\text{H}$ magnetization is aligned along the z-axis during heteronuclear t_2 evolution, one has to shift backwards two proton pulses, the inversion

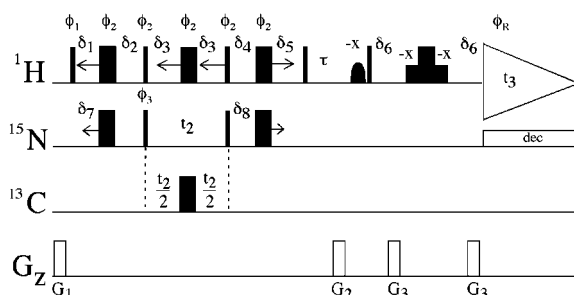


Figure 3. Pulse scheme for the 3D ${}^1\text{H}\text{-}{}^{15}\text{N}$ HSQC-NOESY experiment. Narrow and wide pulses denote 90° flip angles, respectively. Pulse phases are along the x-axis unless indicated otherwise. $\phi_1 = 45^\circ, 45^\circ, 225^\circ, 225^\circ$; $\phi_2 = 135^\circ, 135^\circ, 315^\circ, 315^\circ$; $\phi_3 = 0^\circ, 180^\circ$; $\phi_k = 0^\circ, 180^\circ, 180^\circ, 0^\circ$; neglecting pulse duration in the following: $t_1 = \delta_4 - \delta_5 + t_2 - 2\delta_3 + \delta_2 - \delta_1$; $\Delta t_1 = 1/\text{SW}(\text{F}_1)$; $\Delta t_2 = 1/\text{SW}(\text{F}_2)$ (where SW denotes the sweep width); δ_1 (init.) = δ_2 (init.) = δ_4 (init.) = δ_5 (init.) = δ_7 (init.) = δ_8 (init.) = 2.25 ms; δ_3 (init.) = $t_2/2$; t_2 (init.) = 50 μs ; $\Delta t_1 = \Delta\delta_4 - \Delta\delta_5 = 2\Delta\delta_3 = \Delta\delta_2 - \Delta\delta_1$; $\Delta\delta_5 = -\Delta t_1/2.44$; $\Delta\delta_4 = \Delta\delta_8 = \Delta t_1 + \Delta\delta_5$; $\Delta\delta_3 = -\Delta t_1/2$; $\Delta\delta_1 = -\Delta t_1/(1 + (3.25 + \Delta t_2(1_2 - 1) - t_2)/2.25)$; $\Delta\delta_2 = \Delta t_1 + \Delta\delta_1$; $\Delta\delta_7 = \Delta\delta_1$ for $(\delta_1 + \delta_2) < 5.4$ ms; $\Delta\delta_7 = \Delta\delta_1 + (\Delta\delta_2 + \Delta\delta_1)/2$ for $(\delta_1 + \delta_2) > 5.4$ ms; where t_1 and Δt_1 denote ${}^1\text{H}$ evolution time and its increment, respectively; and analogously for δ_i and $\Delta\delta_i$ with $\Delta\delta_i > 0$ for increment and $\Delta\delta_i < 0$ for decrement; $\Delta\delta_i$ values are functions of the current value of t_2 ; 1_1 and 1_2 are the number of complex data points for ${}^1\text{H}$ (F_1) and ${}^{13}\text{C}$ (F_2), respectively. Gradient pulses are sine-bell shaped with a maximum strength of 20 G/cm and duration: $G_1 = G_2 = 2$ ms; $G_3 = 0.4$ ms.

pulse initially at the centre of t_2 and the following 90° pulse. In doing so, one achieves the gradual insertion of ${}^1\text{H}$ evolution within the currently available t_2 interval. Clearly, the inversion pulse is kept at the centre of the interval in which ${}^1\text{H}$ magnetization is longitudinal to refocus heteronuclear coupling. Once the currently

available t_2 period is ‘used up’, a 360° resulting pulse (90° - 180° - 90°) has been generated, right at the end of the first INEPT period. At this point the latter can also be included as part of the t_1 evolution, by back-shifting the first proton inversion pulse. Therefore the three delays (retro-INEPT, t_2 , initial INEPT) are used one after the other for t_1 monitoring. One should realize that the initial increments of ^1H evolution (first step corresponding to the retro-INEPT) are always executed in the same fashion, independently of the current value of t_2 , whereas the additional increments of t_1 are executed firstly within the t_2 period (itself an incremented delay, second step) and finally, for the amount needed to complete t_1 evolution, by using the initial INEPT delay (third step). Clearly, the progressive overlaying of ^1H and ^{15}N evolution times (during the second step) brings about the generation of multiple quantum coherence (MQ) and therefore from this point of view the experiment appears at that stage as a ‘gradual’ insertion of a portion of an HMQC type of evolution into an HSQC experiment. The extension of ^1H evolution (beyond the time of the retro-INEPT) under the form of MQ, instead of single quantum (SQ) components, turns out to be advantageous in terms of relaxation, if compared with the conventional experiment in which ^1H evolution follows ^{15}N evolution under the form of SQ coherence. In fact, one has to compare the relaxation rate of the MQ coherence (new scheme) with the product of the relaxation rates of the two SQ coherences (conventional scheme) and, since $1/T_{2\text{MQ}} < 1/T_{2\text{H}} + 1/T_{2\text{N}}$ (Bax et al., 1990), one indeed expects an advantage from the new scheme. Moreover, once the available t_2 period is fully included in t_1 , one can use, as a final ‘bonus’, the initial INEPT period to complete ^1H evolution. In practice, the relative advantage of the new method compared to the conventional one depends on the duration selected for ^1H evolution. In the conventional experiment ^1H evolution simply follows ^{15}N evolution in the pulse sequence and typically one would select a shorter evolution for proton, due to its faster decay for T_2 relaxation and homonuclear coupling modulation. In the new scheme homonuclear modulation unavoidably occurs just the same during the MQ period, whereas relaxation is not as fast, as previously stated, and therefore the decay is slower. However, more importantly, such decay occurs in practice only during the t_2 period. Such a period is by definition variable, extending in practice from zero until its maximum value corresponding to the selected duration of ^{15}N evolution.

Let us now put the comparison in more quantitative terms. For simplicity we will consider the two INEPT periods $\delta_1 + \delta_2$ and $\delta_4 + \delta_5$ as constant times. Let us now indicate the additional time in which ^1H magnetization is in the transverse plane (as SQ coherence) with Δt_{1a} (observable signal being S_a) in the conventional experiment. Analogously for Δt_{1b} and S_b in the new experiment. All values of t_1 evolution (longer than the retro-INEPT period $\delta_4 + \delta_5$) are practically executed by setting appropriate values for Δt_{1a} and Δt_{1b} . In general $\Delta t_{1a} > \Delta t_{1b}$.

S_a and S_b are given by the following expressions, where only the relevant relaxation terms are included:

$$S_a = \exp -[(\delta_1 + \delta_2)/T_{2\text{H}}] \exp -(t_2/T_{2\text{N}}) \exp -[(\delta_4 + \delta_5)/T_{2\text{H}}] \exp -(\Delta t_{1a}/T_{2\text{H}}) \quad (1)$$

$$S_b = \exp -[(\delta_1 + \delta_2)/T_{2\text{H}}] \exp -(2\delta_3/T_{2\text{N}}) \exp -[(t_2 - 2\delta_3)/T_{2\text{MQ}}] \exp -[(\delta_4 + \delta_5)/T_{2\text{H}}] \exp -(\Delta t_{1b}/T_{2\text{H}}) \quad (2)$$

The sensitivity gain can now be represented by the ratio

$$S_b/S_a = \exp[(t_2 - 2\delta_3)/T_{2\text{N}}] \exp -[(t_2 - 2\delta_3)/T_{2\text{MQ}}] \exp[(\Delta t_{1a} - \Delta t_{1b})/T_{2\text{H}}] \quad (3)$$

Since $1/T_{2\text{MQ}} < 1/T_{2\text{H}} + 1/T_{2\text{N}}$ one can easily derive the following expression:

$$S_b/S_a > \exp -[(t_2 - 2\delta_3)/T_{2\text{H}}] \exp[(\Delta t_{1a} - \Delta t_{1b})/T_{2\text{H}}] \quad (4)$$

This expression holds in general for any combination of t_1 and t_2 values. Nevertheless, it is instructive to distinguish three different situations.

(a) $t_2 + \delta_1 + \delta_2 < \Delta t_{1a}$. In this case $\delta_3 = 0$ and $\Delta t_{1b} = \Delta t_{1a} - (t_2 + \delta_1 + \delta_2)$. $S_b/S_a > \exp[(\delta_1 + \delta_2)/T_{2\text{H}}] > 1$. The first INEPT period ($\delta_1 + \delta_2$) is fully exploited for ^1H evolution.

(b) $t_2 < \Delta t_{1a} < t_2 + \delta_1 + \delta_2$. In this case $\delta_3 = 0$ and $\Delta t_{1b} = 0$. $S_b/S_a > \exp[(\Delta t_{1a} - t_2)/T_{2\text{H}}] > 1$. ^1H evolution is not sufficiently long to cover completely the first INEPT period. Therefore the delay ($\delta_1 + \delta_2$) is only partially exploited.

(c) $t_2 > \Delta t_{1a}$. In this case $\delta_3 = (t_2 - \Delta t_{1a})/2$ and $\Delta t_{1b} = 0$. $S_b/S_a > 1$. ^1H evolution is completely covered by the t_2 period. Therefore the delay ($\delta_1 + \delta_2$) is

not exploited and the gain just depends on the slightly more favourable relaxation occurring during the time ($t_2 - 2\delta_3$).

In any case the real advantage of the new experiment can clearly be measured by the relative portion of relaxation-free delay (the initial INEPT) that finally enters in ^1H evolution. For short durations of the ^1H evolution time (up to 8 or 10 ms) this would not occur for the entire experiment but only for the initial increments of the t_2 period, until the t_2 duration completely covers the t_1 extension. For longer ^1H evolution of course the advantage would extend longer. For ^1H evolution times as long as the sum of the maximum t_2 period plus the INEPT and retro-INEPT periods ($t_2 \text{ max} + 11 \text{ ms}$) the advantage would be present for the entire experiment (i.e. for all current values of t_2). In this respect one could conclude that while it might appear somewhat tricky to make the best choice for the total duration of ^1H evolution, it nevertheless holds true for any given choice that the new experiment is advantageous with respect to the conventional one. In practice, although one might be tempted to select for ^1H t_1 evolution the time previously indicated ($\text{max } t_2 + 11 \text{ ms}$), as in fact we have done in the example reported below, due consideration should be given to the possibility that such a long time could well be too penalizing for fast decaying proton signals.

Similar arguments to those illustrated previously for the pulse sequence of Figure 1, relative to the modification of the line shape induced by the new type of t_1 - t_2 acquisition, apply also to the pulse scheme shown in Figure 3. The advantage of the reduced T_2 relaxation losses translates again via a change of the theoretical Lorentzian peak shape in enhanced signal to noise ratios. In this experiment the modification of the peak shape is somewhat ill defined since the signal decay during t_1 incrementation is subject to different regimes, firstly with no relaxation losses (retro-INEPT period), secondly relaxing like a component of multiple quantum proton-nitrogen (t_2 period, of variable duration following t_2 incrementation), and finally again with no relaxation losses or with a reduced relaxation rate, if ^1H evolution extends beyond the duration of the initial INEPT. In practice, though, the effect is finally detected in terms of enhanced sensitivity, as previously reported, particularly after signal apodization.

The result is illustrated in Figure 4. Here cross sections are reported at different nitrogen-proton chemical shifts obtained with the conventional (a, b, c) and the new (d, e, f) pulse sequence. (For the sake of com-

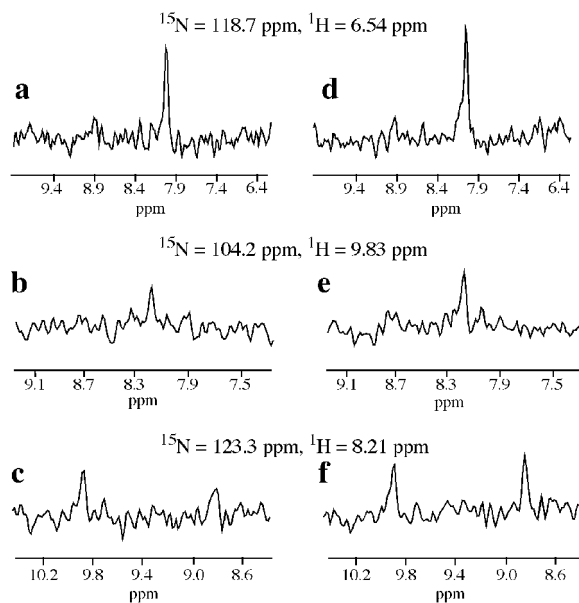


Figure 4. F_3 cross sections selected at the indicated $^1\text{H}(F_1)$ and $^{15}\text{N}(F_2)$ chemical shifts extracted from the 3D data sets obtained with the conventional pulse sequence (a, b, c) and with the new scheme (d, e, f), respectively. Total evolution times: ^1H $t_1 = 27.8 \text{ ms}$; ^{15}N $t_2 = 16.8 \text{ ms}$. In both t_1 and t_2 dimensions a shifted ($\pi/3$) sine-bell shaped weighting function has been applied prior to FT transformation. NOESY mixing time $\tau = 100 \text{ ms}$.

parison one could take Figure 3 to represent also the conventional sequence simply by considering the first two proton inversion pulses as fixed at the center of the corresponding intervals, $\delta_1 + \delta_2$ and $\delta_3 + \delta_3$, respectively, during the semi-constant time incrementation of the retro-INEPT preceding NOE mixing (Grzesiek et al., 1995).) The spectra were recorded on the same sample as before. The experiment duration was 20 h. Proton T_2 values are typically in the range of 5–20 ms and the resulting gains vary accordingly from 5% to 60%, again more pronounced for more critical signals. Pulse phases are arranged to allow radiation damping to restore water magnetization along the z-axis at the end of the NOESY mixing time (Lippens et al., 1995), before the final WATERGATE flip-back pulses (Grzesiek and Bax, 1993). The observed signals are the amide protons.

As for the practical implementation of the two experiments, the corresponding pulse sequences are written in the Bruker standard pulse program language. Each pulse scheme is programmed as a single experiment. The variation of the delays employed in the proton channel is not implemented using fixed increments (or decrements) as in conventional schemes,

but for each new t_2 value the appropriate delays are redefined according to the rationale of the experiments. The practical rules are given in the figure legends. A series of logical 'if statements' and 'variable' statements allows the continuous readjustment of the different delays during the execution of the experiment. For the sake of clarity one should also notice that the time incrementation is executed differently for the two sequences. In the pulse scheme of the 3D ^1H - ^{13}C HMQC-NOESY (Figure 1) the time incrementation of t_1 evolution is accomplished by the simultaneous redefinition of the delays δ_1 , δ_2 , δ_3 , δ_4 , and δ_6 for each value of the evolution time t_2 . In the pulse scheme of the 3D ^1H - ^{15}N HSQC NOESY (Figure 3) the time incrementation for t_1 evolution has to take place in separate steps. Firstly the delays δ_4 , δ_5 and δ_8 are used until δ_5 approaches zero and the entire interval $\delta_4 + \delta_5$ from an initial value of 4.5 ms approaches 5.5 ms. Secondly the delays δ_3 are used. From an initial value equal to $t_2/2$ they are decreased until they approach zero. Thirdly the delays δ_1 , δ_2 and δ_7 are used to complete t_1 evolution. The increment or decrement values for these delays depend on the current and maximum values of the time t_2 . The pulse program handles the execution of the pulse sequence as a single experiment to ensure that no discontinuity in signal amplitude is occurring. The practical rules are given in the figure legend.

A limitation inherent in the new pulse schemes that should not be overlooked lies precisely in the fact that during the time in which ^1H and heteronuclear chemical shift evolutions are overlaid no proton-heteronucleus decoupling can be implemented. Therefore for NH_2 groups and methylenes (CH_2) and methyl (CH_3) systems the trick does not apply, since the loss due to direct passive couplings with additional protons would largely obscure the gain provided by the decreased apparent relaxation rate. However, the two new schemes may replace the conventional ones as building blocks in the corresponding 3D and 4D experiments in all applications involving the indirect monitoring of spin pairs as crucial as amide NH groups, or aromatic and alpha CH groups in proteins. For such systems, particularly for ^1H T_2 relaxation times of the order of a few milliseconds, which is the case for several proteins that can be approached by NMR, the sensitivity gain one can achieve with the new schemes can be remarkable. Clearly, the natural comparison to be made in terms of sensitivity is with the analogous experiments based on the TROSY technique (Pervushin et al., 1997, 1998), particularly for

amide NH groups and aromatic CH groups in large proteins, for which a sufficiently strong TROSY effect is expected at the appropriate magnetic fields. The TROSY experiment inherently follows an HSQC type of scheme, since it relies on the selective detection of the slowly relaxing components of heteronuclear single quantum coherences. Clearly our trick of overlaying proton and heteronuclear evolutions does not apply to TROSY sequences, since the introduction of proton-heteronuclear multiple quantum coherences would simply defeat the rationale on which TROSY is based. Therefore the two techniques represent two alternative methods to monitor such systems. Their relative sensitivity clearly depends on the interplay of several parameters like T_2 relaxation times, chemical shift anisotropies, dipolar couplings and magnetic field strengths, and it can only be assessed on a case by case basis.

Supplementary material

The pulse programs of the two experiments illustrated in Figures 1 and 3 are available upon request from the corresponding author. They are encoded using standard AVANCE Bruker software. Detailed experimental parameters are also available.

Acknowledgements

We thank P. Neddermann and S. Sambucini for the protein sample preparation.

References

- Barbato, G., Cicero, D.O., Nardi, C., Steinkühler, C., Cortese, R., De Francesco, R. and Bazzo, R. (1999) *J. Mol. Biol.*, **289**, 371–384.
- Bax A., Ikura, M., Kay, L.E., Torchia, D.A. and Tschudin, R. (1990) *J. Magn. Reson.*, **86**, 304–318.
- Fesik, S.W. and Zuiderweg, E.R.P. (1988) *J. Magn. Reson.*, **78**, 588–593.
- Grzesiek, S. and Bax, A. (1993) *J. Biomol. NMR*, **3**, 185–204.
- Grzesiek, S., Wingfield, P., Stahl, S., Kaufman, J.D. and Bax, A. (1995) *J. Am. Chem. Soc.*, **117**, 9594–9595.
- Lee, W., Revington, M.J., Arrowsmith, C. and Kay, L.E. (1994) *FEBS Lett.*, **350**, 87–90.
- Pervushin, K., Riek, R., Wider, G. and Wüthrich, K. (1997) *Proc. Natl. Acad. Sci. USA*, **94**, 12366–12371.
- Pervushin, K., Riek, R., Wider, G. and Wüthrich, K. (1998) *J. Am. Chem. Soc.*, **120**, 6394–6400.
- Vuister, G.W., Clore, G.M., Gronenborn, A.M., Powers, R., Garrett, D.S., Tschudin, R. and Bax, A. (1993) *J. Magn. Reson.*, **B101**, 210–213.